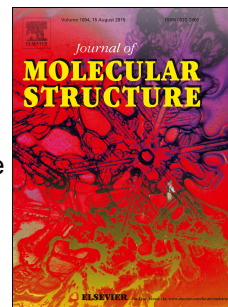


Accepted Manuscript

Structural characterization of benzoyl-1*H*-pyrazole derivatives obtained in lemon juice medium: Experimental and theoretical approach

Vesna Milovanović, Zorica D. Petrović, Slađana Novaković, Goran A. Bogdanović, Dušica Simijonović, Vladimir P. Petrović



PII: S0022-2860(19)30665-9

DOI: <https://doi.org/10.1016/j.molstruc.2019.05.095>

Reference: MOLSTR 26602

To appear in: *Journal of Molecular Structure*

Received Date: 6 March 2019

Revised Date: 10 May 2019

Accepted Date: 22 May 2019

Please cite this article as: V. Milovanović, Z.D. Petrović, Slađ. Novaković, G.A. Bogdanović, Duš. Simijonović, V.P. Petrović, Structural characterization of benzoyl-1*H*-pyrazole derivatives obtained in lemon juice medium: Experimental and theoretical approach, *Journal of Molecular Structure* (2019), doi: <https://doi.org/10.1016/j.molstruc.2019.05.095>.

This is a PDF file of an unedited manuscript that has been accepted for publication. As a service to our customers we are providing this early version of the manuscript. The manuscript will undergo copyediting, typesetting, and review of the resulting proof before it is published in its final form. Please note that during the production process errors may be discovered which could affect the content, and all legal disclaimers that apply to the journal pertain.

Graphical abstract

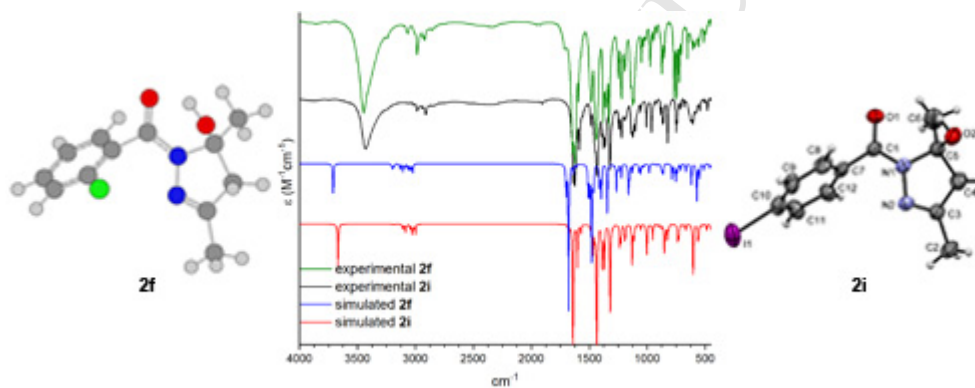
Structural characterization of benzoyl-1*H*-pyrazole derivatives obtained in lemon juice medium: experimental and theoretical approach

Vesna Milovanović,^a Zorica D. Petrović,^{*a} Slađana Novaković,^b Goran A. Bogdanović,^b Dušica Simijonović,^a and Vladimir P. Petrović^a

^aUniversity of Kragujevac, Faculty of Science, Department of Chemistry, R. Domanovića 12, 34000 Kragujevac, Serbia.

^bVinča Institute of Nuclear Sciences, University of Belgrade, P.O. Box 522, 11001 Belgrade, Serbia.

Corresponding author: *Z. Petrović: tel.: +381-34-336-223; +381-34-335-039; e-mail: zorica.petrovic@pmf.kg.ac.rs



Structural characterization of benzoyl-1*H*-pyrazole derivatives obtained in lemon juice medium: experimental and theoretical approach

Vesna Milovanović,^a Zorica D. Petrović,^{*a} Slađana Novaković,^b Goran A. Bogdanović,^b Dušica Simijonović^a, and Vladimir P. Petrović^a

^aUniversity of Kragujevac, Faculty of Science, Department of Chemistry, R. Domanovića 12, 34000 Kragujevac, Serbia.

^bVinča Institute of Nuclear Sciences, University of Belgrade, P.O. Box 522, 11001 Belgrade, Serbia.

Abstract

Simple, one-pot, and low-cost reactions of acetylacetone with a variety of substituted benzoyl hydrazides in lemon juice, as eco-friendly medium, were performed. In reactions of benzoyl hydrazides with electron-donating groups on phenyl ring, the 1-benzoyl-1*H*-pyrazole derivatives were obtained in short reaction time, and in good to high yields. On the other hand, benzoyl hydrazides with electron-withdrawing groups reacted slower, yielding the mixture of 1-benzoyl-5-hydroxy-4,5-dihydro-1*H*-pyrazole and benzoyl-1*H*-pyrazole derivatives. It is worth pointing out that two products, (2-chlorophenyl)(4,5-dihydro-5-hydroxy-3,5-dimethylpyrazol-1-yl)methanone and (4-iodophenyl)(3,5-dimethyl-1*H*-pyrazol-1-yl)methanone are reported here for the first time. All obtained compounds were characterized using IR, UV-Vis and NMR, experimentally and theoretically, as well as with melting points. Good agreement between experimental and simulated IR, UV-Vis, ¹H and ¹³C NMR spectra was achieved. In addition, crystal structures and Hirshfeld surfaces analysis of (4,5-dihydro-5-hydroxy-3,5-dimethylpyrazol-1-yl)(4-iodophenyl)methanone were reported.

Keywords: Spectral characterisation, Crystal structure, Density functional theory, Green synthetic procedure

Corresponding author:

*Z. Petrović: tel.: +381-34-336-223; +381-34-335-039; e-mail: zorica.petrovic@pmf.kg.ac.rs

1. Introduction

Nitrogen-containing heterocycles attract the attention of the researchers during decades. These compounds present very interesting pharmacophores and building blocks for compounds with biological or clinical interest. Heterocycles with pyrazolo moiety are often an integral part of medically interesting compounds. Pyrazolo-containing heterocycles have been applied as commercially available drugs such as Celecoxib (anti-inflammatory drug),[1] Zoniporide (cardioprotective drug),[2] Fezolamine (antidepressant).[3] In addition, these compounds express antimicrobial,[4,5]

antiproliferative,[6,7] antitubercular,[8] antiangiogenic,[9] analgesic,[7,10] anticonvulsant,[11] hypoglycemic,[12] anxiolytic,[13] and antiviral activity.[14,15]

According to their multifaceted activities, compounds with pyrazolo moiety are constituents of agro-chemicals, such as herbicides (pyrazolynate, topramezone, azimsulfuron), fungicides (furametpyr, bixafen, pyraclostrobin), insecticides (fenpiclonil, tricyclazole, fipronil).[16] The pyrazoles are important intermediates in organic chemistry[17] and useful ligands in coordination chemistry.[18,19] As one of the most flexible nitrogen donor heterocycles, pyrazoles can be easily incorporated into polydentate ligand structures.[18,20] There are several methods for the synthesis of pyrazoles, such as: reaction of chalcones and hydrazines,[21,22] coupling of hydrazine, aldehyde and ethyl acetoacetate,[23] the Knorr hydrazine condensation with 1,3-dicarbonyles or their derivatives,[24–29]. In addition, Suzuki–Miyaura cross-coupling reactions are powerful tool for the synthesis of pyrazole derivatives.[30] These reactions are often performed at elevated temperature in organic solvents, and in the presence of different harmful catalysts.[28–31]

Many analytical techniques, such as NMR, IR, UV-Vis, X-ray, ESI-MS, etc., as well as quantum chemical calculations, have been developed to elucidate physico-chemical properties of these compounds. Further, Hirshfeld surface analysis (HSA) is a powerful tool for the analysis of intermolecular interactions within their crystal packing. [21,32,33] Herein, we report a simple and low-cost protocol, where freshly squeezed lemon juice was used as catalyst and solvent in one-pot synthesis of benzoyl-1*H*-pyrazole derivatives. All synthesized compounds were experimental characterized using IR, UV-Vis, ¹H and ¹³C NMR spectroscopy. Density functional theory (DFT) was used to perform the geometry optimization and calculations of the NMR, IR, and UV-Vis electronic spectra of the investigated compounds. X-ray determination and analysis of Hirshfeld surfaces in the solved crystal structure were presented, also. To the best of our knowledge, the literature fails with data related to the usage of lemon juice, as natural, recyclable and eco-friendly medium for their synthesis,[34,35] as well as data for synergistic experimental and theoretical approach to the elucidation of their structure.

2. Experimental

All the chemicals were procured from either Sigma-Aldrich Co. or Merck & Co. The IR spectra were recorded on a Perkin-Elmer Spectrum One FT-IR spectrometer using the KBr plates. The UV/Vis spectra were measured at room temperature within the 200-500 nm range on the Agilent Technologies, Cary 300 Series UV-Vis Spectrophotometer. A solution of 2.5×10^{-5} M of each compound was prepared in methanol and then 2 mL of the corresponding solution was injected into the 10 mm quartz cell and recorded spectrum. The ¹H NMR and ¹³C NMR spectra were run on a Varian Gemini spectrometer (200 MHz and 50 MHz for ¹H and ¹³C respectively) using CDCl₃ as solvent. Melting points were

determined on a Mel-Temp capillary melting points apparatus, model 1001. Elemental microanalysis for carbon, hydrogen, and nitrogen were performed at the Faculty of Chemistry, University of Belgrade. Lemon was purchased from local market.

2.1. Preparation of lemon juice

Lemon was squeezed, and obtained juice was filtered through Büchner funnel with a sintered glass disc in order to remove pulp. The pH value of the filtrate was about 2. The obtained juice was then used in the reaction.

2.2. General procedure for the synthesis of benzoyl-1H-pyrazole derivatives **2** and **3**

A mixture of acetylacetone (1 mmol) and corresponding hydrazide (1 mmol) in lemon juice (3 ml) was stirred at room temperature. Reaction progress was monitored using thin layer chromatography (TLC). In case where reaction product precipitated during reaction, the mixture was filtered and washed with water, without further purification. In cases where mixture of two products were obtained, as well as when substances were liquid, reaction mixture was dissolved in ethyl acetate and washed with water, and products were separated by column chromatography. All products (**2f-j** and **3a-j**) were characterized with melting points, ¹H NMR, ¹³C NMR and IR spectra. For the new compounds **2f** and **3i** purity was confirmed by elemental analysis, and corresponding spectral data are presented here, while for other compounds corresponding data are presented in Supplementary material).

2.3. Spectral characterization of benzoyl-1H-pyrazole derivatives

(2-chlorophenyl)(4,5-dihydro-5-hydroxy-3,5-dimethylpyrazol-1-yl)methanone

(2f): White powder (10%); Eluent: dichloromethane/ethyl acetate (3:1); mp 95-97 °C; ¹H NMR (200 MHz, CDCl₃) δ: 1.95 (s, 3H), 1.99 (s, 3H), 2.98 (AB-q, Δv_{AB} = 51.7 Hz, J = 18.4 Hz, 2H), 4.85 (s, 1H), 7.44 – 7.29 (m, 4H), ¹³C NMR (50 MHz, CDCl₃) δ: 16.11, 26.67, 51.56, 92.00, 126.40, 128.35, 129.30, 130.30, 131.02, 135.70, 155.80, 166.49; IR (KBr): ν_{max} = 3445, 3067, 2985, 2856, 1643, 1623, 1441, 1378, 1221, 1125, 1050, 975, 874, 746, cm⁻¹; C₁₂H₁₃ClN₂O₂ (FW = 252.7): C, 57.04; N, 11.09; H, 5.19%; found: C, 57.20; N, 11.12; H, 5.20%

(4-iodophenyl)(3,5-dimethyl-1H-pyrazol-1-yl)methanone (**3i**):

Yellow solid (36%); Eluent: dichloromethane/ethyl acetate (2:1); mp 65-67 °C; ¹H NMR (200 MHz, CDCl₃) δ: 2.25 (s, 3H), 2.63 (s, 3H), 6.07 (s, 1H), 7.72 (d, J = 8.5 Hz, 2H), 7.83 (d, J = 8.4 Hz, 2H); ¹³C NMR (50 MHz, CDCl₃) δ: 13.88, 14.35, 100.07, 111.24, 128.72, 132.70, 137.03, 145.10, 152.33, 167.52; IR (KBr): ν_{max} = 2924, 1694, 1583, 1376, 1352, 1008, 918, 833, 769, 742, 623 cm⁻¹; C₁₂H₁₁IN₂O (FW = 326.14): C, 44.19; N, 8.59; H, 3.40%; found: C, 44.03; N, 8.56; H, 3.41%.

2.4. X-ray crystal structure determination

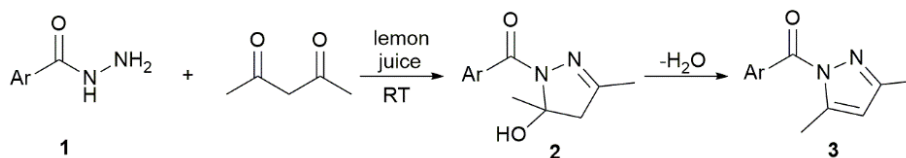
Single-crystal X-ray diffraction data for compound **2i** were collected at an Oxford Gemini S diffractometer, using monochromatized MoK α radiation ($\lambda = 0.71073 \text{ \AA}$). Data reduction and empirical absorption correction were performed with CrysAlisPRO [36]. The structure was solved by direct methods using SHELXS and refined on F^2 by full-matrix least-squares using SHELXL [37]. All non-hydrogen atoms were refined anisotropically. H atoms bonded to C atoms were placed in geometrically calculated positions and refined using the riding model with U_{iso} values constrained to $1.2U_{\text{eq}}$ or $1.5U_{\text{eq}}$ of the parent C atoms. H atom bonded to O atom was constrained in position found from a difference Fourier synthesis. The PLATON [38] software was used to perform geometrical calculation and the Mercury [39] was employed for molecular graphics. In order to identify the relative importance of the intermolecular interactions within the crystal packing of **2i** the Hirshfeld surface analysis was performed by using CrystalExplorer[40]. The molecular Hirshfeld surface d_{norm} was mapped over a fixed colour scale: -0.53 (red) to 1.41 \AA (blue). Crystallographic details are summarized in Table S1. Crystallographic data have been deposited with the Cambridge Structural Database, CCDC deposition numbers 1887548.

2.5. Density functional theory calculations

The Gaussian 09 program package was used to perform all calculations.[41] The equilibrium geometries of all compounds were calculated using the B3LYP-D3 functional in conjunction with the 6-311+G(d,p) basis set,[42,43] in the gas-phase and chloroform ($\epsilon = 24.3$) since it was used as solvent for experimental NMR spectra, using the conductor-like solvation model (CPCM) as implemented in Gaussian09.[44–46] To confirm that all structures are local minima, frequency calculations were done. The optimized geometries in the gas-phase were used for simulation of IR spectra, while the NMR shifts for all hydrogen and carbon atoms relative to TMS were calculated using the Gauge-Independent Atomic Orbital (GIAO) method. UV–Vis spectra were simulated using TD-DFT and structures optimized in methanol, because experimental spectra were acquired using this solvent. It is worth pointing out that simulated IR bands were not scaled, since obtained bands are in good agreement with experimental ones. On the other hand, simulated NMR chemical shifts, both hydrogen and carbon, were scaled using scaling factors obtained using the least squares method and amount 0.9639 and 0.9422.

3. Results and discussion

In continuation of our interest on synthesis of nitrogen heterocyclic compounds,[47,48] new green synthesis of benzoyl-1*H*-pyrazole derivatives under mild reaction conditions was achieved. The synthesis was performed in the presence of freshly squeezed lemon juice as solvent and natural source of citric acid, i.e. Bronsted acid catalyst (pH \sim 2), Scheme 1.



Scheme 1. General reaction for the synthesis of benzoyl-1*H*-pyrazole derivatives in lemon juice.

3.1. Synthesis of 1-benzoyl-1*H*-pyrazole derivatives

To optimize reaction conditions, model reaction between benzohydrazide (1 mmol) and acetylacetone (1 mmol) in different amounts of lemon juice was performed at room temperature, Table 1. Initially, in the presence of 1 and 1.5 mL of juice and after 3 h, corresponding product was formed in moderate yield. Higher amount of juice (2 and 2.5 mL) increased the yield and reduced reaction time. In 3 mL of lemon juice, the yield of the product was very good and reaction time shorter. Further increase of the lemon juice to 4 mL didn't affect the yield and reaction time. The formation of the pyrazole product **3** was tested in pure water, also. The product was obtained in low yield and after prolongation of the reaction time to 24 h (Table 1, entry 8). However, this reaction mixture contained final pyrazole product **3**, as well as its precursor 1-benzoyl-5-hydroxy-4,5-dihydro-1*H*-pyrazole **2** in 5:4 ratio. Moreover, to test the influence of temperature on the dehydration of **2**, the reaction mixture was heated to reflux, Table 1 entry 9. After 5 hours of heating, the yield of **3** was improved to 70%, while amount of **2** was only 2%.

Table 1. Optimisation of the reaction conditions^a.

Entry	Lemon juice/water (mL)	Time (h)	Yield (%)
1	1	3	65
2	1.5	3	70
3	2	1.5	75
4	2.5	1.5	85
5	3	1	90
6	4	1	90
7	5	1	90
8 ^b	3	24	47
9 ^c	3	5	70

^aReaction conditions: benzohydrazide (1 mmol) and acetylacetone (1 mmol), room temperature; ^{b,c}reactions performed in water, ^broom temperature; ^creflux.

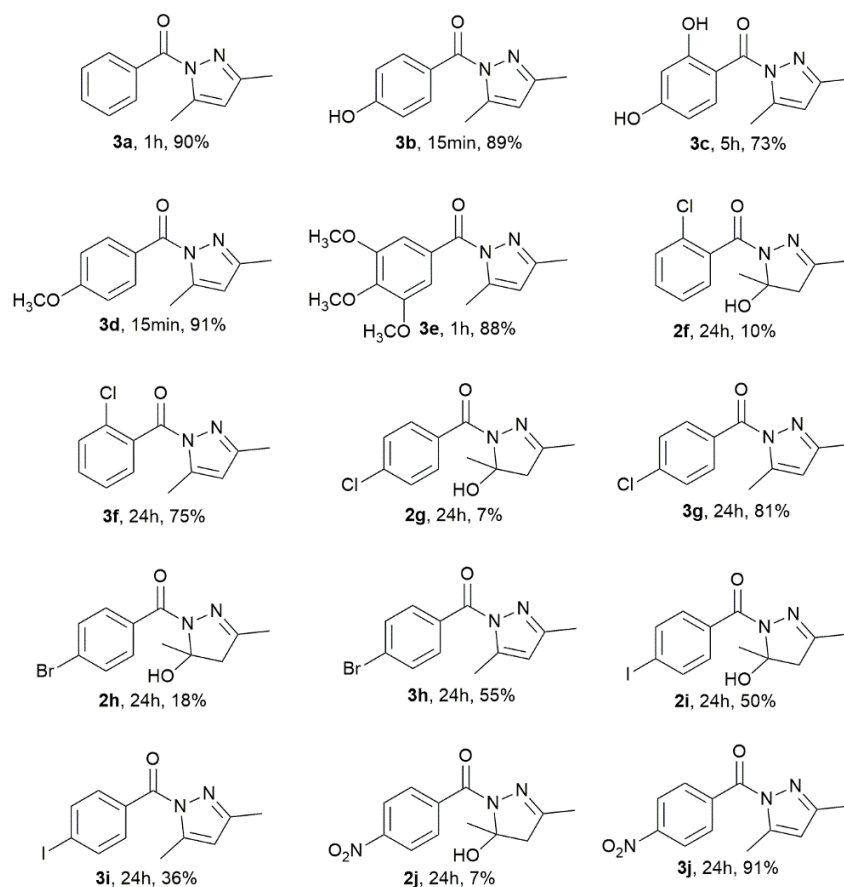
Considering obtained results, 3 mL of lemon juice was used as optimal for the synthesis of 1-benzoyl-1*H*-pyrazoles derivatives starting from aromatic hydrazides **1a-j** and acetylacetone in molar ratio 1:1, Scheme 1. It is important to emphasize that, some of the reactions with substituted benzoyl hydrazides (**1b** and **1d**) finished much faster than the control reaction with benzohydrazide **1a**. Namely, these reactions finished after 15 minutes, with only final pyrazole products **3** present in the reaction mixtures, Table 2. Therefore, we performed all reactions for the synthesis of pyrazole derivatives for 15 minutes in 3 mL of lemon juice, starting from hydrazides **1a-j** and acetylacetone in molar ratio 1:1.

Table 2. Product distribution (**2:3**) of the reactions of different benzoyl hydrazides (**1a-j**) with acetylacetone after 15 minutes.

Compound	Yield (%)	
	2	3
a	18	72
b	/	89
c	/	42
d	/	91
e	18	74
f	36	46
g	42	19
h	46	15
i	77	2
j	88	4

In the cases where benzoyl hydrazides with electron-donating groups on phenyl ring **1b** and **1d** reacted with acetylacetone, only the 1-benzoyl-1*H*-pyrazoles derivatives **3b** and **3d** were obtained in high yields. On the other hand, benzohydrazides **1a** and **1e**, as well as benzoyl hydrazides with electron-withdrawing groups **1f-j** reacted slower, yielding the mixture of the corresponding 1-benzoyl-5-hydroxy-4,5-dihydro-1*H*-pyrazoles **2** and final products 1-benzoyl-1*H*-pyrazoles **3**.

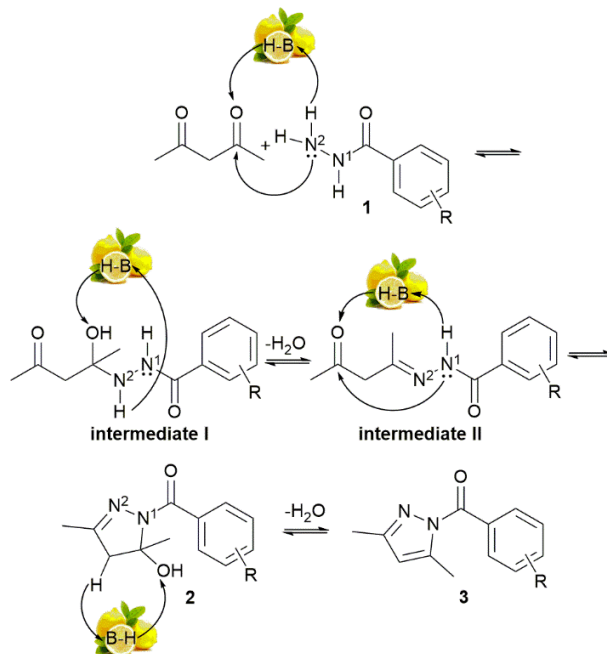
To improve yields, reaction time was prolonged, Scheme 2. Products **3b** and **3d** were obtained in high yields after 15 minutes and increase of reaction time didn't influence any increase in yields of these products. Reactions where hydrazides **1a** and **1e** were used, finished after 1 hour, and products were obtained in very good yield. On the other hand, reactions with hydrazides **1c** and **1f-j** required prolongation of the reaction time, Scheme 2.



Scheme 2. Products obtained in reactions of aromatic hydrazides with acetylacetone at room temperature in lemon juice.

To get further insight in the reaction, and to find reasonable explanation for the distribution of the products **2** and **3**, mechanism of this reaction is proposed and analysed, Scheme 3. The reaction starts with concerted protonation of diketone with HB (in our case citric acid), followed with nucleophilic attack of nitrogen N^2 from **1** to the carbonyl group of acetylacetone, and deprotonation of the same N^2 . This way formed intermediate **I** undergoes dehydration in similar fashion. Here, HB from lemon juice protonates OH group forming water molecule, with simultaneous deprotonation of N^2 . Hydrazido-imine intermediate **II** is formed. Next, remaining carbonyl group of intermediate **II** is subjected to protonation, while the N^1 is being deprotonated. In the same time, 1-benzoyl-5-hydroxy-4,5-dihydro-1*H*-pyrazoles **2** is formed, as product of cyclocondensation reaction. Dehydration of **2** would be facilitated with the presence of citric acid. This agrees with the fact that uncatalyzed test reaction in water produced high amount of **2**, while the presence of acid from lemon juice significantly favoured dehydration of **2** to form final product **3**. In addition, dehydration process is dependent on the electron density on N^1 .^[49,50] This process would be favoured with increased electron density on N^1 , since this would make aromatisation of the ring easier. Our results show that electron-donating

groups positioned on the aromatic ring of the benzoyl hydrazide enable quick formation of the final pyrazole adduct **3**, while electron accepting groups decrease electron density on N¹ and therefore make this process slower.



Scheme 3. The suggested mechanism for the formation of 1-benzoyl-1*H*-pyrazole derivatives.

3.2. Structural characterization of 1-benzoyl-1*H*-pyrazole derivatives

All synthesized compounds were characterized using spectroscopic techniques such as IR, UV-Vis, ¹H and ¹³C NMR spectroscopy, as well as with melting points. Two of fifteen obtained derivatives are newly synthesized compounds (**2f** and **3i**). The purity of newly synthesized compounds was confirmed and by elemental analysis. In addition, the structure of compound **2i** was confirmed by single-crystal X-ray diffraction analysis. To our best knowledge, the crystal structure of that compound has not been reported so far.

Experimental and simulated IR spectra of 1-benzoyl-5-hydroxy-4,5-dihydro-1*H*-pyrazole derivatives **2f** and **2i**, as well as of 1-benzoyl-1*H*-pyrazole **3i** are presented in Fig. 1, while all other spectra are given in Figs. S3 and S4. To assign experimental bands, IR spectra were simulated using DFT. One can note that all simulated spectra are very similar to those experimentally obtained. Here, IR spectral characterization of compounds **2f**, **2i**, and **3i** will be discussed. Deeper insight in experimental and simulated spectra of **2i** and **3i** revealed difference in their structure. Particularly, the band at 3429 cm⁻¹ present in the spectrum of **2i** is absent from the spectrum of **3i**, suggesting that the OH group in compound **3i** is not present. Vibration around 1630 cm⁻¹ in the spectrum of **2i** is redshifted to 1690 cm⁻¹ in the spectrum of **3i** and corresponds to C=O vibration, while C-N vibrations from the spectrum of **2i** are blueshifted from 1433 and 1376 cm⁻¹ to 1376 and 1273 cm⁻¹ in the spectrum of **3i**. Bands around 1323, 1221, 1125, 964, 824, and 605 cm⁻¹ are present only in the spectrum of **2i** and correspond to CH₂ deformational vibration, C-O, N-C(OH), C-OH, C-CH₂, and O-H out of plane deformational vibrations,

respectively. In the spectra of **3i**, bands around 917 and 833 cm^{-1} correspond to Ar–C–C=O and =C–H deformational out of plane vibrations. Although Ar–C–C=O system is present in **2i**, the band of this vibration is most probably absent from spectra due to stabilization through C=O...H–O hydrogen bonding. In both spectra, bands around 1580, 1480, 1010, and 745 cm^{-1} are present, and correspond to aromatic C–C, CH₃ deformational, aromatic C–I vibration, and aromatic deformational out of plane C–H vibrations, respectively. IR spectra of **2f** and **2i** are mutually very similar. The only difference between these spectra is that vibration corresponding to aromatic carbon halogen vibration is redshifted to 1125 cm^{-1} in the spectra of **2f**.

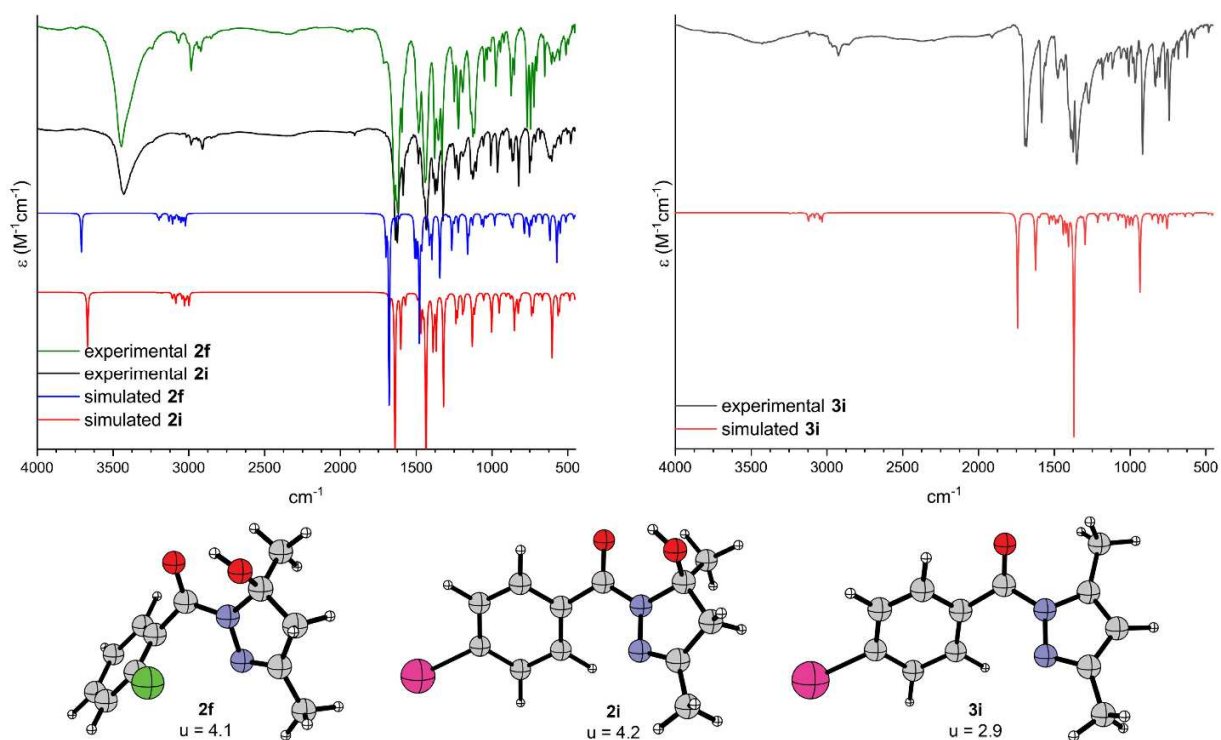


Fig. 1. Optimised structures, dipole moment values of compounds **2f**, **2i**, and **3i**, as well as their experimental and simulated IR spectra.

All compounds were characterised using experimental and theoretical ¹H and ¹³C NMR spectra. Chemical shifts of 1-benzoyl-5-hydroxy-4,5-dihydro-1*H*-pyrazole derivatives **2f** and **2i**, as well as of 1-benzoyl-1*H*-pyrazole **3i** are presented in Tables 3 and 4, while the corresponding data for other compounds are given in Tables S2 and S3.

The ¹H NMR spectra of compounds **2f** and **2i** reveal that there is no pronounced difference in chemical shifts, except in the aromatic region, Table 3. In both experimental spectra two diastereotopic protons of methylene group (H_a and H_b) of pyrazole ring resonate as AB quartets at 2.98 ppm ($J_{AB} = 18.4$ Hz and $\Delta\nu_{AB} = 51.7$ Hz) and 2.96 ppm with ($J_{AB} = 18.4$ Hz and $\Delta\nu_{AB} = 47.4$ Hz). These diastereotopic protons undergo spin–spin coupling to each other, Fig. 2. In simulated spectra these signals appear at 2.96 and 2.91 ppm. Singlets of methyl groups attached to C3 and C5 of the pyrazole ring appear at 1.95 and 1.99 ppm (1.78 and 1.94 ppm simulated) in the spectrum of **2f**, and at 1.96 and 2.04

ppm (1.84 and 1.99 ppm simulated) in the spectrum of **2i**. Singlets for hydroxy group bonded to stereocenter C5 appear at 4.85 and 5.00 ppm in corresponding spectrum of each compound, while in predicted spectra at 4.51 and 4.88 ppm. The aromatic protons of **2f** are observed as multiplet at 7.37 ppm (simulated 7.33 ppm), while in the spectra of **2i** they are observed as doublets at 7.85 and 8.07 ppm (simulated 7.57 and 7.78 ppm). In the ^1H NMR spectrum of dehydrated product **3i** singlet originating from proton bonded to C4 carbon of pyrazole ring appear at 6.07 ppm (simulated 6.10 ppm). Methyl groups attached to C3 and C5 carbons of pyrazole ring are presented with two sharp singlets resonating at 2.25 and 2.63 ppm (simulated 2.26 and 2.62 ppm), and protons of phenyl group as doublets at 7.72 and 7.83 ppm (simulated 7.62 and 7.86 ppm).

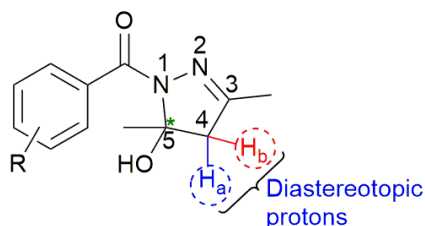


Fig. 2. Skeleton of compounds **2**.

Table 3. Experimental and simulated ^1H NMR chemical shifts (ppm).

	2f		2i		3i	
	exp	sim	exp	sim	exp	sim
CH ₃	1.99	1.94	2.04	1.99	2.25	2.26
	1.95	1.78	1.96	1.84	2.63	2.62
C4-H	/	/	/	/	6.07	6.10
C4-H _a , H _b	2.98	2.96	2.96	2.91	/	/
Ar	7.37	7.33	7.85	7.57	7.72	7.62
			8.07	7.78	7.83	7.86
C5-OH	4.85	4.51	5.00	4.88	/	/

In ^{13}C NMR spectra of compounds **2f** and **2i** carbon atoms of methyl groups appear around 16 and 27 ppm in both experimental and simulated spectra, Table 4, Fig. S5. Peaks around 156, 51, and 93 ppm originate from C3, C4, and C5 carbons (in simulated spectra 159, 53, and 95 ppm), respectively. Carbons of C=O group appeared around 167 ppm. Similarly, to the case of ^1H NMR spectra, the only difference between ^{13}C NMR spectra of compounds **2f** and **2i** is in the aromatic region. Namely, there are six peaks in the spectrum of **2f** in region of 126-136 ppm, while in the spectrum of **2i**, owing to *p*-substitution of I atom, there are four signals in the range of 98-137 ppm. In the spectrum of compound **3i**, both methyl groups appeared around 14 ppm (simulated 15 and 17 ppm), and carbon atoms C3, C4, and C5 around 152, 100, and 145 ppm (simulated 153, 111, and 147 ppm), respectively. Aromatic carbons were observed in the region 111-137 ppm (simulated 132-138 ppm), and carbon of carbonyl group around 167 ppm (simulated 166). It is worth pointing out that simulated ^1H and ^{13}C spectra reproduced chemical shifts with high accuracy. Namely, average absolute errors (AAE) amount 0.13 and 1.69 ppm, while

the correlation coefficients (R) for the dependencies of the calculated chemical shifts on the experimental values are larger than 0.99, Tables S2 and S3, Fig. S5.

Table 4. Experimental and simulated ^{13}C NMR chemical shifts (ppm).

	2f		2i		3i	
	exp	sim	exp	sim	exp	sim
CH ₃	16.11	18.17	16.20	18.06	13.85	15.61
	26.67	26.71	26.87	26.42	14.34	16.15
C4-H	/		/		111.20	110.82
C4-H _a , H _b	51.56	52.87	51.02	52.72	/	
C5	92.00	94.75	92.79	94.73	145.10	147.15
C3	155.80	159.46	155.59	157.76	152.33	153.39
C=O	166.49	164.49	167.52	165.95	167.52	165.69
Ar	131.02	136.72	133.64	133.32	128.72	132.36
	135.70	138.27	131.39	131.11	132.70	132.44
	129.30	128.05	136.86	134.50	137.03	134.48
	130.30	129.09	98.30	109.26	111.24	118.68
	126.40	126.01				
	128.35	127.26				

In addition to the IR and NMR spectral characterization, UV-Vis spectra of the compounds **2f**, **2i**, and **3i** were acquired and simulated, Fig. 3. In both, experimental and simulated spectra of compounds **2f**, **2i**, and **3i**, one major absorption band appeared. In experimental spectra of **2f**, **2i**, and **3i** absorption bands appear at 230, 251, and 263 nm, respectively. In the simulated spectra of **2f**, major band is somewhat blueshifted to 227 nm, while in the case of **2i** and **3i**, bands are redshifted and appear at 277.5 and 288 nm. To distinguish the parts of molecules responsible for electronic transitions, Kohn-Sham orbitals were constructed, Figs. S6, S7, and S8. Experimental band at 230 nm (simulated 227 nm) in the spectrum of **2f** is consequence of HOMO to LUMO+2 electron transition. On molecular level, electron transition from pyrazole moiety of the molecule to the benzoyl group is responsible for the appearance of this band. In the spectrum of **2i**, band at 251 nm is a consequence of electron transition from HOMO to LUMO (from almost entire molecule to the benzoyl part of the molecule), with some participation of HOMO-1 (benzoyl part of the molecule) and HOMO-4 (pyrazole part) to the LUMO (benzoyl part) electron transitions. In the case of **3i**, besides HOMO to LUMO transition (from benzoyl to benzoyl part of the molecule), there is some contribution from HOMO-2 to LUMO electron transition (from pyrazole part to the benzoyl part of the molecule). Considering regions responsible for the appearance of the bands in the spectra of **2f**, **2i**, and **3i** at 230, 251, and 263 nm, respectively, it is clear that the highest energy band at 230 nm is consequence of electron transition between different parts of the molecule (large spatial gap), while in the cases of 251 and 263 nm, these bands are caused with smaller spatial gap electron transitions within the same region of **2i** and **3i** molecules.

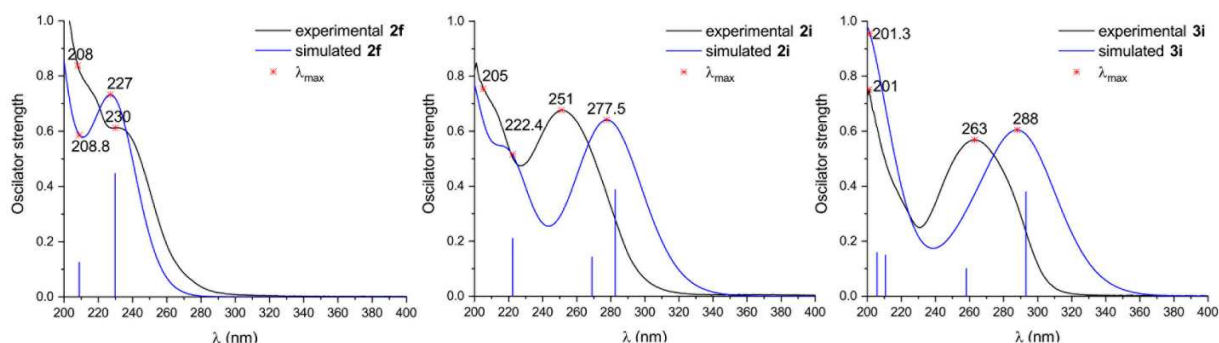


Fig. 3. Experimental and simulated UV-Vis spectra of **2f**, **2i**, and **3i**.

Solid-state structure of **2i** was determined by single crystal X-ray diffraction. The molecular structure is shown in Fig. 4, while the selected geometry parameters are given in Table 5. It is worth pointing out, that there is very good agreement between X-ray diffraction geometrical parameters and those obtained from the gas phase optimized structure of **2i**. The pyrazoline ring in **2i** displays expected deviation from planarity, caused by the presence of two sp^3 hybridized C atoms (r.m.s 0.0757 Å). The ring adopts an envelope conformation, where the C5 atom, carrier of the methyl and hydroxyl substituents, deviates for -0.28 (1) Å from the least-squares plane of the remaining N1/N2/C3/C4 atoms (r.m.s 0.004 Å). Similar to previously reported 4,5-dihydro-1*H*-pyrazole derivatives,[51–54] the N2–C3 bond [1.2786(17) Å] has the shortest length, indicating a localization of electron density in this part of the ring.

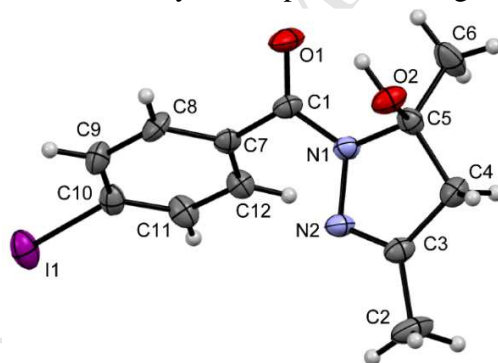


Fig. 4. Molecular structure and atom-labeling scheme of **2i** with displacement ellipsoids drawn at the 30% probability level.

Table 5. Selected X-ray and calculated bond lengths (Å) and angles (°) of **2i**.

	X-ray	calculated AAE=0.013		X-ray	calculated AAE=0.5
N1–N2	1.406(8)	1.392	N1–N2–C3	106.7(6)	108.6
N1–C5	1.471(9)	1.501	N2–N1–C5	112.5(5)	112.8
N2–C3	1.283(10)	1.280	N1–C5–C4	100.5(6)	100.8
C3–C4	1.492(12)	1.506	N2–C3–C4	114.2(7)	114.1
C4–C5	1.518(11)	1.538	N1–C1–C7	119.4(5)	120.0
N1–C1	1.364(9)	1.369	N1–C1–O1	119.3(6)	119.3
C1–O1	1.239(9)	1.234	C3–C4–C5	103.0(6)	103.4
C1–C7	1.484(11)	1.493			

The molecule displays E configuration with regard to N1–C1 bond [1.364(9) Å], as evidenced by the torsion angle N2–N1–C1–O1 of 161.4(7)°. The mean plane defined by atoms N1/C1/O1/C7/ makes a smaller dihedral angle with the mean plane of pyrazoline ring [12.5(5)°] in comparison to the dihedral angle toward the phenyl ring [48.1(3)°]. These values suggest that the interrupted delocalization within the pyrazoline favors a delocalization of N2 free electron pair towards the carbonyl group adjacent to the ring. This is also reflected in N1–C1 bond which is notably shorter than analogue bond in 1-benzoyl-5-hydroxy-4,5-dihydro-1*H*-pyrazole derivatives. The dihedral angle between the mean planes of pyrazoline ring and phenyl ring is 58.1(3)°.

The molecular structure is stabilized by intramolecular hydrogen bond formed between hydroxyl group and carbonyl O acceptor [O2–H2...O1: H...O 2.50 Å O–H...O 123°]. In the crystal packing the same donor and acceptor are involved in the formation of specific O2–H...O1 centrosymmetric dimer [O2–H2...O1ⁱ: H...O 2.04 Å O–H...O 150°, (i) = -x, -y, -z+1]. The similar motif has been observed in previously literature data[53,54]. The dimers interconnect by weak C–H...O interaction [C4–H4b...O2ⁱⁱ: H...O 2.57 Å C–H...O 145°, (ii) = x, -y+1, -z+1] into a chain extending along the *b* axis, Fig. 3. The N2 acceptor of **2i** has no role in hydrogen bonding. The crystal structure of **2i** is further stabilized only by weakly attractive interactions arising from the van der Waals contacts.

Hirshfeld surface analysis (Figure 6) has been used to quantify the intermolecular interactions stabilizing the crystal packing of **2i**. [40] The deep red spots on Hirshfeld surface indicate the shortest contacts in the **2i** system result from dominant O2–H2...O1 hydrogen bond (Figure 6a). In the corresponding 2D fingerprint plot (Figure 6b) this centrosymmetric interaction is indicated by a pair of distinct spikes. The percentage contribution of the O...H interactions to the crystal packing is only 14.0%, while the main contribution results from the H...H contacts (44.1%). The majority of Hirshfeld surface area of **2i** is characterized by light colors indicating the prevalence of weak van der Waals and electrostatic contacts (Figure 6a and Figure S1). Short lateral spikes in 2D fingerprint plot reflect the weak H...I contacts which contribute to the Hirshfeld surface with 15.4%. In the crystal packing each iodine atom fits into the fold of a neighboring molecule (Figure S2) resulting in weak van der Waals interactions. The distance between the iodine and the centroid of phenyl ring is 3.799(3) Å.

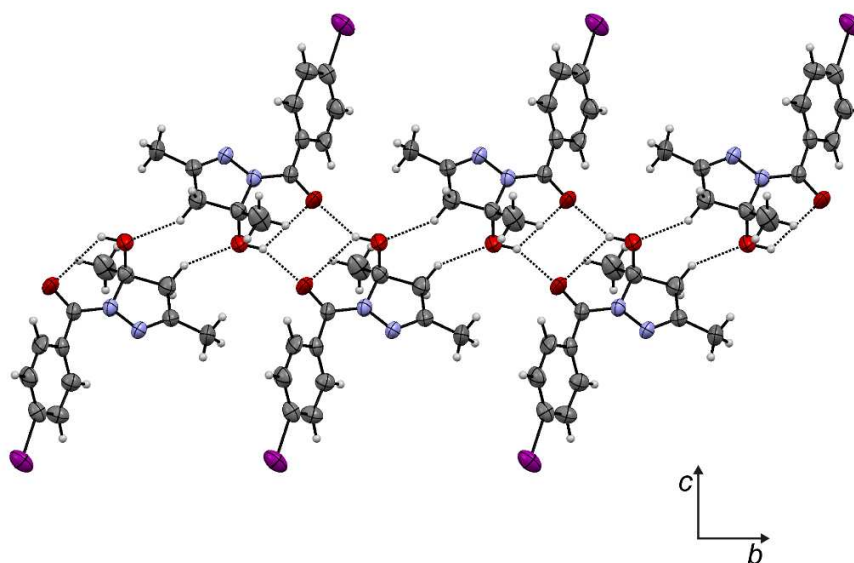


Fig. 5. The chain of centrosymmetric O–H...O bonded dimers of **2i**.

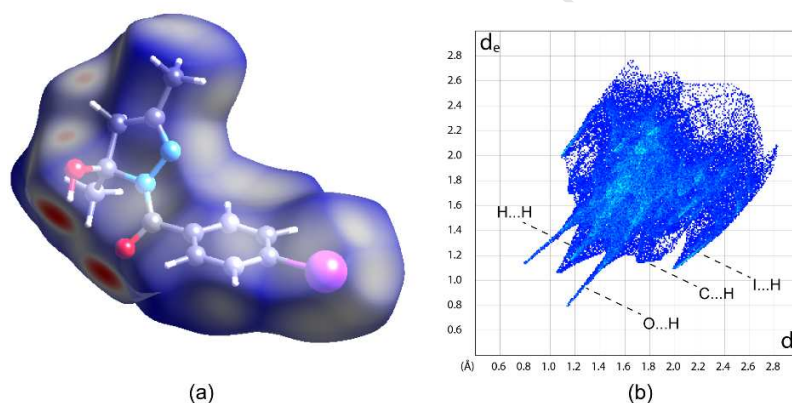


Fig. 6. (a) Hirshfeld surface of **2i**; (b) two-dimensional fingerprint plot.

4. Conclusion

A new green method for the synthesis of benzoyl-1*H*-pyrazole derivatives was performed in lemon juice as eco-friendly medium and biocatalyst. Reaction of benzoyl hydrazides with acetylacetone produced 1-benzoyl-5-hydroxy-4,5-dihydro-1*H*-pyrazoles **2** and 1-benzoyl-1*H*-pyrazoles **3**, depending on the hydrazide substitution. Benzoyl hydrazides with electron-withdrawing groups reacted slower, yielding the mixture of **2** and **3**. Electron-donating substituted benzoyl hydrazides reacted faster, yielding only pyrazole products **3** in high yields. Two compounds, **2f** and **3i**, and their structures are reported here for the first time. IR, NMR, and UV-Vis spectral characterization was done experimentally, as well as theoretically. All simulated spectra agree with the experimental ones. Solid-state structures of **2i** was determined using single crystal X-ray diffraction analysis. The molecule **2i** displays E configuration described by the

torsion angle N2–N1–C1–O1 of 161.4(7)°. The N1–C1 bond length of 1.364(9) Å as well as the dihedral angle between N1/C1/O1/C7/ fragment and pyrazoline ring of 12.5(5)° suggest the delocalization of the electron density from the pyrazoline N2 toward the carbonyl group. In the crystal packing the molecules of 2i form O2–H...O1 hydrogen bonded centrosymmetric motif characteristic for 1-benzoyl-5-hydroxy-4,5-dihydro-1*H*-pyrazole derivatives. Hirshfeld surface analysis indicates the prevalence of weak van der Waals and electrostatic contacts in stabilization of crystal packing, with small participation of hydrogen bonds.

Acknowledgements

This investigation was supported by the Ministry of Education, Science and Technological Development of the Republic of Serbia project No. 172016 and 172014.

- [1] K.R.A. Abdellatif, M.T. Elsaady, S.A. Abdel-Aziz, A.H.A. Abusabaa, Synthesis, cyclooxygenase inhibition and anti-inflammatory evaluation of new 1,3,5-triaryl-4,5-dihydro-1*H*-pyrazole derivatives possessing methanesulphonyl pharmacophore, *J. Enzyme Inhib. Med. Chem.* 31 (2016) 1545–1555. doi:10.3109/14756366.2016.1158168.
- [2] W.R. Tracey, M.C. Allen, D.E. Frazier, A.A. Fossa, C.G. Johnson, R.B. Marala, D.R. Knight, A. Guzman-Perez, Zoniporide: A Potent and Selective Inhibitor of the Human Sodium-Hydrogen Exchanger Isoform 1 (NHE-1), *Cardiovasc. Drug Rev.* 21 (2006) 17–32. doi:10.1111/j.1527-3466.2003.tb00103.x.
- [3] E.R. Baizman, A.M. Ezrin, R.A. Ferrari, D. Luttinger, Pharmacologic profile of fezolamine fumarate: a nontricyclic antidepressant in animal models., *J. Pharmacol. Exp. Ther.* 243 (1987) 40–54. doi:10.1016/j.synthmet.2010.02.034.
- [4] N.M.M. Hamada, E.M. Sharshira, Synthesis and Antimicrobial Evaluation of Some Heterocyclic Chalcone Derivatives, *Molecules.* 16 (2011) 2304–2312. doi:10.3390/molecules16032304.
- [5] E.M. Sharshira, N.M.M. Hamada, Synthesis and in Vitro Antimicrobial Activity of Some Pyrazolyl-1-carboxamide Derivatives, *Molecules.* 16 (2011) 7736–7745. doi:10.3390/molecules16097736.
- [6] E.M. Perchellet, M.M. Ward, A.-L. Skaltsounis, I.K. Kostakis, N. Pouli, P. Marakos, J.-P.H. Perchellet, Antiproliferative and proapoptotic activities of pyranoxanthenones, pyranothioxanthenones and their pyrazole-fused derivatives in HL-60 cells., *Anticancer Res.* 26 (2004) 2791–804. <http://www.ncbi.nlm.nih.gov/pubmed/15136638>.
- [7] V. Kumar, V. Sareen, V. Khatri, S. Sareen, Recent Applications of Pyrazole and its Substituted Analogs, *Int. J. Appl. Rea.* 2 (2016) 461–469.
- [8] U. Pandit, A. Dodiya, Synthesis and antitubercular activity of novel pyrazole–quinazolinone hybrid analogs, *Med. Chem. Res.* 22 (2013) 3364–3371. doi:10.1007/s00044-012-0351-0.
- [9] A.H. Abadi, A.A.H. Eissa, G.S. Hassan, Synthesis of Novel 1,3,4-Trisubstituted Pyrazole Derivatives and Their Evaluation as Antitumor and Antiangiogenic Agents, *Chem. Pharm. Bull. (Tokyo).* 51 (2003) 838–844. doi:10.1248/cpb.51.838.
- [10] S. Ailawadi, Jyoti, M. Yadav, D. Pathak, Synthesis and characterization of some substituted pyrazoles as analgesics and anti inflammatory agents, *Der Pharma Chem.* 3 (2011) 215–222. doi:<http://scholarsresearchlibrary.com/archive.html>.

- [11] M. Abdel-Aziz, G.E.-D.A. Abu-Rahma, A.A. Hassan, Synthesis of novel pyrazole derivatives and evaluation of their antidepressant and anticonvulsant activities, *Eur. J. Med. Chem.* 44 (2009) 3480–3487. doi:10.1016/j.ejmech.2009.01.032.
- [12] E. Hernández-Vázquez, R. Aguayo-Ortiz, J.J. Ramírez-Espinosa, S. Estrada-Soto, F. Hernández-Luis, Synthesis, hypoglycemic activity and molecular modeling studies of pyrazole-3-carbohydrazides designed by a CoMFA model, *Eur. J. Med. Chem.* 69 (2013) 10–21. doi:10.1016/j.ejmech.2013.07.054.
- [13] R. Dnyanpeeth, Synthesis and Pharmacological Activities of 4-carboxaldehyde and Its Aldimines Derivatives, *Asian J. Chem.* 20 (2008) 5037–5045.
- [14] G. Ouyang, Z. Chen, X. Cai, B. Song, P.S. Bhadury, S. Yang, L. Jin, W. Xue, D. Hu, S. Zeng, Synthesis and antiviral activity of novel pyrazole derivatives containing oxime esters group, *Bioorg. Med. Chem.* 16 (2008) 9699–9707. doi:10.1016/j.bmc.2008.09.070.
- [15] O.I. El-Sabbagh, M.M. Baraka, S.M. Ibrahim, C. Pannecouque, G. Andrei, R. Snoeck, J. Balzarini, A.A. Rashad, Synthesis and antiviral activity of new pyrazole and thiazole derivatives, *Eur. J. Med. Chem.* 44 (2009) 3746–3753. doi:10.1016/j.ejmech.2009.03.038.
- [16] C. Lamberth, Pyrazole Chemistry in Crop Protection, *Heterocycles*. 71 (2007) 1467. doi:10.3987/REV-07-613.
- [17] V. Kumar, K. Kaur, G.K. Gupta, A.K. Sharma, Pyrazole containing natural products: Synthetic preview and biological significance, *Eur. J. Med. Chem.* 69 (2013) 735–753. doi:10.1016/j.ejmech.2013.08.053.
- [18] H. Willms, W. Frank, C. Ganter, Coordination Chemistry and Catalytic Application of Bidentate Phosphaferrocene–Pyrazole and –Imidazole Based P,N-Ligands, *Organometallics*. 28 (2009) 3049–3058. doi:10.1021/om8012025.
- [19] M.A. Halcrow, Pyrazoles and pyrazolides—flexible synthons in self-assembly, *Dalt. Trans.* 9226 (2009) 2059. doi:10.1039/b815577a.
- [20] F. Mohr, E. Cerrada, M. Laguna, Synthesis and coordination chemistry of an alkyne functionalised bis(pyrazolyl)methane ligand, *Dalt. Trans.* 35 (2006) 5567. doi:10.1039/b613311h.
- [21] K. Kumara, A.D. Kumar, S. Naveen, K.A. Kumar, N.K. Lokanath, Synthesis, spectral characterization and X-ray crystal structure studies dihydro-1H-pyrazole-1-carboxamide: Hirshfeld surface, DFT and thermal analysis, *J. Mol. Struct.* 1161 (2018) 285–298. doi:10.1016/j.molstruc.2018.02.068.
- [22] M. Gurumurthy, S. Bharath, A. Dileep, S. Naveen, N. Krishnappagowda, B. Ningappa, K. Ajay, Bioorganic Chemistry Design and environmentally benign synthesis of novel thiophene appended pyrazole analogues as anti-inflammatory and radical scavenging agents: Crystallographic, in silico modeling, docking and SAR characterization, *Bioorg. Chem.* 73 (2017) 109–120. doi:10.1016/j.bioorg.2017.06.004.
- [23] K. Kumari, D.S. Raghuvanshi, V. Jouikov, K.N. Singh, Sc(OTf)₃-catalyzed, solvent-free domino synthesis of functionalized pyrazoles under controlled microwave irradiation, *Tetrahedron Lett.* 53 (2012) 1130–1133. doi:10.1016/j.tetlet.2011.12.094.
- [24] Z. Wang, Knorr Pyrazole Synthesis, in: *Compr. Org. Name React. Reagents*, John Wiley & Sons, Inc., Hoboken, NJ, USA, 2010: pp. 1631–1633. <http://doi.wiley.com/10.1002/0471704156.ch7>.
- [25] Y.O. Ko, Y.S. Chun, C.-L. Park, Y. Kim, H. Shin, S. Ahn, J. Hong, S. Lee, An effective and general method for the highly regioselective synthesis of 1-phenylpyrazoles from β -enaminoketoesters, tandem Blaise–acylation adducts, *Org. Biomol. Chem.* 7 (2009) 1132.

- doi:10.1039/b820324e.
- [26] Z.-X. Wang, H.-L. Qin, Solventless syntheses of pyrazole derivatives Electronic supplementary information (ESI) available: analytical and spectroscopic data. See <http://www.rsc.org/suppdata/gc/b3/b312833d/>, *Green Chem.* 6 (2004) 90. doi:10.1039/b312833d.
- [27] S. Fustero, R. Román, J.F. Sanz-Cervera, A. Simón-Fuentes, A.C. Cuñat, S. Villanova, M. Murguía, Improved Regioselectivity in Pyrazole Formation through the Use of Fluorinated Alcohols as Solvents: Synthesis and Biological Activity of Fluorinated Tebufenpyrad Analogs, *J. Org. Chem.* 73 (2008) 3523–3529. doi:10.1021/jo800251g.
- [28] M. Curini, O. Rosati, V. Campagna, F. Montanari, G. Cravotto, M. Boccalini, Layered Zirconium Sulfophenyl Phosphonate as Heterogeneous Catalyst in the Synthesis of Pyrazoles and 4,5,6,7-Tetrahydro-1(2) H -indazoles, *Synlett.* 2005 (2005) 2927–2930. doi:10.1055/s-2005-921904.
- [29] H. Emtiazi, M.A. Amrollahi, B.B.F. Mirjalili, Nano-silica sulfuric acid as an efficient catalyst for the synthesis of substituted pyrazoles, *Arab. J. Chem.* 8 (2015) 793–797. doi:10.1016/j.arabjc.2013.06.008.
- [30] K.M. Clapham, A.S. Batsanov, M.R. Bryce, B. Tarbit, Trifluoromethyl-substituted pyridyl- and pyrazolylboronic acids and esters: synthesis and Suzuki–Miyaura cross-coupling reactions, *Org. Biomol. Chem.* 7 (2009) 2155. doi:10.1039/b901024f.
- [31] V. Polshettiwar, R.S. Varma, Greener and rapid access to bio-active heterocycles: room temperature synthesis of pyrazoles and diazepines in aqueous medium, *Tetrahedron Lett.* 49 (2008) 397–400. doi:10.1016/j.tetlet.2007.11.017.
- [32] K. Kumara, N. Shivalingegowda, L.D. Mahadevaswamy, A.K. Kariyappa, N.K. Lokanath, PT, *Chem. Data Collect.* (2016). doi:10.1016/j.cdc.2016.11.006.
- [33] K. Kumara, M. Jyothi, N. Shivalingegowda, S.A. Khanum, L.N. Krishnappagowda, US CR, *Chem. Data Collect.* (2017). doi:10.1016/j.cdc.2017.06.003.
- [34] H. Sachdeva, D. Dwivedi, P. Goyal, Green Chemical Synthesis and Analgesic Activity of Fluorinated Thiazolidinone, Pyrazolidinone, and Dioxanedione Derivatives, *Org. Chem. Int.* 2013 (2013) 1–8. doi:10.1155/2013/976032.
- [35] L.D. Mahadevaswamy, A.K. Kariyappa, An Environmentally Benign Lemon Juice Mediated Synthesis of Novel Furan Conjugated Pyrazole Derivatives and Their Biological Evaluation, *Pharm. Chem. J.* 51 (2017) 670–677. doi:10.1007/s11094-017-1672-6.
- [36] Rigaku Oxford Diffraction, CrysAlisPro Software system, Rigaku Corporation, Oxford, UK, 2015.
- [37] G.M. Sheldrick, Crystal structure refinement with SHELXL, *Acta Crystallogr. Sect. C Struct. Chem.* 71 (2015) 3–8. doi:10.1107/S2053229614024218.
- [38] A.L. Spek, Single-crystal structure validation with the program PLATON, *J. Appl. Crystallogr.* 36 (2003) 7–13. doi:10.1107/S0021889802022112.
- [39] C.F. Macrae, P.R. Edgington, P. McCabe, E. Pidcock, G.P. Shields, R. Taylor, M. Towler, J. van de Streek, Mercury: visualization and analysis of crystal structures, *J. Appl. Crystallogr.* 39 (2006) 453–457. doi:10.1107/S002188980600731X.
- [40] M.A.S. S. K. Wolff, D. J. Grimwood, J. J. McKinnon, M. J. Turner, D. Jayatilaka, *CrystalExplorer ver. 3.1.*, (2013).
- [41] E.G.S. M. J. Frisch, W. G. Trucks, B. H. Schlegel, V.B. A. M. Robb, R. J. Cheeseman, G. Scalmani, M.C. B. Mennucci, A. G. Petersson, H. Nakatsuji, K.T. X. Li, P. H. Hratchian, F. A. Izmaylov, J. Bloino, G. Zheng, L. J. Sonnenberg, M. Hada, M. Ehara, Y.H. R.

- Fukuda, J. Hasegawa, M. Ishida, T. Nakajima, A.J.M.J. O. Kitao, H. Nakai, T. Vreven, J.J.H. E. J. Peralta, F. Ogliaro, M. Bearpark, R.K. E. Brothers, N. K. Kudin, N. V. Staroverov, C.J.B. J. Normand, K. Raghavachari, A. Rendell, J.M.M. S. S. Iyengar, J. Tomasi, M. Cossi, N. Rega, C.A. M. Klene, J. E. Knox, J. B. Cross, V. Bakken, O.Y. J. Jaramillo, R. Gomperts, E. R. Stratmann, W.J.O. J. A. Austin, R. Cammi, C. Pomelli, A.G.V. L. R. Martin, K. Morokuma, G. V. Zakrzewski, D.A.D. P. Salvador, J. J. Dannenberg, S. Dapprich, J.C. and O. Farkas, B. J. Foresman, V. J. Ortiz, J.D. Fox, Gaussian 09 Rev C, Gaussian Inc., (2009).
- [42] W.Y. and R.G.P. C. Lee, No Title, *Phys. Rev. B Condens. Matter Mater. Phys.* 37 (1988) 785.
- [43] A.D. Becke, A.D. Becke, *Densityfunctional thermochemistry . III . The role of exact exchange Density-functional thermochemistry . III . The role of exact exchange*, 5648 (1993). doi:10.1063/1.464913.
- [44] V.B. and M. Cossi, No Title, *J. Phys. Chem. A.* 102 (1998) 1995–2001.
- [45] B. V. Cossi M, Rega N, Scalmani G, *Energies, structures, and electronic properties of molecules in solution with the C-PCM solvation model.*, *J. Comput. Chem.* 24 (2003) 669–681. doi:10.1002/jcc.10189.
- [46] F. Weigend, R. Ahlrichs, *Balanced basis sets of split valence, triple zeta valence and quadruple zeta valence quality for H to Rn: Design and assessment of accuracy*, *Phys. Chem. Chem. Phys.* 7 (2005) 3297. doi:10.1039/b508541a.
- [47] Z.D. Petrović, D. Simijonović, J. Đorović, V. Milovanović, Z. Marković, V.P. Petrović, *One-Pot Synthesis of Tetrahydropyridine Derivatives: Liquid Salt Catalyst vs Glycolic Acid Promoter. Structure and Antiradical Activity of the New Products*, *ChemistrySelect.* 2 (2017) 11187–11194. doi:10.1002/slct.201701873.
- [48] D. Simijonović, Z.D. Petrović, V.M. Milovanović, V.P. Petrović, G.A. Bogdanović, *A new efficient domino approach for the synthesis of pyrazolyl-phthalazine-diones. Antiradical activity of novel phenolic products*, *RSC Adv.* 8 (2018) 16663–16673. doi:10.1039/C8RA02702A.
- [49] H.G. Bonaccorso, H. Lewandowski, R.L. Drekenner, M.B. Costa, C.M.P. Pereira, A.D. Wastowski, C. Peppe, M.A.P. Martins, N. Zanatta, *Reactions of β -methoxyvinyl trifluoromethyl ketones with 2-pyridinecarboxamidrazone*, *J. Fluor. Chem.* 122 (2003) 159–163. doi:10.1016/S0022-1139(03)00057-5.
- [50] M. a P. Martins, C.M.P. Pereira, S. Moura, G.F. Fiss, C.P. Frizzo, D.J. Emmerich, N. Zanatta, H.G. Bonaccorso, and *Their Application To a One-Pot Synthesis of Azoles*, 2006 (2006) 187–194.
- [51] Y. Chen, D.-C. Li, Y. Zhu, D.-Q. Wang, *5-Hydroxy-1-(3-hydroxy-2-naphthoyl)-3,5-dimethyl-2-pyrazoline*, *Acta Crystallogr. Sect. E Struct. Reports Online.* 64 (2008) o1629–o1629. doi:10.1107/S1600536808023027.
- [52] M. Arfan, M.N. Tahir, R. Khan, S. Saba, M.S. Iqbal, *(2-Aminophenyl)[(5 S)-5-hydroxy-3,5-dimethyl-4,5-dihydro-1 H -pyrazol-1-yl]methanone*, *Acta Crystallogr. Sect. E Struct. Reports Online.* 65 (2009) o1834–o1835. doi:10.1107/S1600536809026294.
- [53] T. Sedaghat, Y. Ebrahimi, L. Carlucci, D.M. Proserpio, V. Nobakht, H. Motamedi, M.R. Dayer, *Diorganotin(IV) complexes with 2-furancarboxylic acid hydrazone derivative of benzoylacetone: Synthesis, X-ray structure, antibacterial activity, DNA cleavage and molecular docking*, *J. Organomet. Chem.* 794 (2015) 223–230. doi:10.1016/j.jorganchem.2015.06.034.

- [54] M.A.P. Martins, D.N. Moreira, C.P. Frizzo, P.T. Campos, K. Longhi, M.R.B. Marzari, N. Zanatta, H.G. Bonacorso, X-ray structure, semi-empirical MO calculations and π -electron delocalization of 1-cyanoacetyl-5-trifluoromethyl-5-hydroxy-4,5-dihydro-1H-pyrazoles, *J. Mol. Struct.* 969 (2010) 111–119. doi:10.1016/j.molstruc.2010.01.050.

ACCEPTED MANUSCRIPT

Highlights

Green synthesis of benzoyl-1*H*-pyrazole derivatives

Experimental and theoretical spectral characterization of pyrazole derivatives

Crystal structure determination

ACCEPTED MANUSCRIPT